UC Berkeley

UC Berkeley Previously Published Works

Title

Case Studies of Forest Windthrows and Mesoscale Convective Systems in Amazonia

Permalink

https://escholarship.org/uc/item/1c5902q3

Journal

Geophysical Research Letters, 50(12)

ISSN

0094-8276

Authors

Feng, Yanlei
Negrón-Juárez, Robinson I
Chiang, John CH
et al.

Publication Date

2023-06-28

DOI

10.1029/2023gl104395

Copyright Information

This work is made available under the terms of a Creative Commons Attribution License, available at https://creativecommons.org/licenses/by/4.0/

Peer reviewed

eScholarship.org Powered by the California Digital Library
University of California

Check for updates

Geophysical Research Letters

RESEARCH LETTER
10.1029/2023GL104395

Case Studies of Forest Windthrows and Mesoscale Convective Systems in Amazonia

Yanlei Feng[1], **Robinson I. Negrón-Juárez**[2], **John C. H. Chiang**[1], **and Jeffrey Q. Chambers**[1,2]

[1]Department of Geography, University of California, Berkeley, CA, USA, [2]Climate and Ecosystem Sciences Division, Lawrence Berkeley National Laboratory, Berkeley, CA, USA

Key Points:

- The storm passing time of mesoscale convective systems (MCSs) is positively correlated with the size of windthrows
- MCSs with colder cloud top temperature are associated with larger size of windthrows
- No significant relationship is found between maximum precipitation intensity and the area of windthrows

Supporting Information:

Supporting Information may be found in the online version of this article.

Correspondence to:

Y. Feng,
ylfeng@berkeley.edu

Citation:

Feng, Y., Negrón-Juárez, R. I., Chiang, J. C. H., & Chambers, J. Q. (2023). Case studies of forest windthrows and mesoscale convective systems in Amazonia. *Geophysical Research Letters*, *50*, e2023GL104395. https://doi.org/10.1029/2023GL104395

Received 25 MAY 2022
Accepted 8 JUN 2023

Author Contributions:

Conceptualization: Yanlei Feng, Robinson I. Negrón-Juárez, Jeffrey Q. Chambers
Data curation: Yanlei Feng
Formal analysis: Yanlei Feng
Funding acquisition: Jeffrey Q. Chambers
Investigation: Yanlei Feng
Methodology: Yanlei Feng, Robinson I. Negrón-Juárez, Jeffrey Q. Chambers
Software: Yanlei Feng
Supervision: Robinson I. Negrón-Juárez, John C. H. Chiang, Jeffrey Q. Chambers
Visualization: Yanlei Feng
Writing – original draft: Yanlei Feng

© 2023. The Authors.
This is an open access article under the terms of the Creative Commons Attribution License, which permits use, distribution and reproduction in any medium, provided the original work is properly cited.

Abstract This study identifies 38 cases of windthrows in the Amazonia to explore the relationship between windthrows and the characteristics (storm passing time, cloud top temperature, and maximum precipitation) of mesoscale convective systems (MCSs) that produced them. Most of windthrow cases in this study occurred in August and September. The storm passing time is positively correlated with the size of windthrows. MCSs with colder cloud top temperature (with a mean at 206 K)—indicating deeper convection—resulted in large windthrows, while those with warm cloud top (with a mean above 230 K) resulted in relatively small windthrows except for windthrows in the western Amazonia. No significant relationship is found between maximum precipitation intensity and the area of windthrows.

Plain Language Summary Fan-shaped dead forest patches were found over the entire Amazonia. These patches affect the role the Amazon forests played in the world's carbon cycle. Scientists found that frequent thunderstorms result in these dead forest patches, but how does the process happen? In this study, we explored the three characteristics of thunderstorms, including their passing over time, cloud top temperature, and associated precipitation, to identify their relationship with the size of the dead forests. We found that long-lived thunderstorms with thicker and tall clouds, providing more power to the mesoscale convective systems, result in bigger sizes of dead forest patches. Moreover, forests in the western Amazonia are more vulnerable to thunderstorms than forests on the other parts of the Amazonia.

1. Introduction

Tropical forests absorb about 12%–15% of anthropogenic carbon emissions and play significant roles in balancing the global carbon cycle (Esquivel-Muelbert et al., 2020; Mitchard, 2018). However, tropical forests can become a major carbon source under climate change (Baccini et al., 2017; Cox et al., 2013; Gatti et al., 2021). Forest disturbances increase the uncertainty of tropical forest carbon cycle response (Baldocchi, 2008; Chambers et al., 2013; Knohl et al., 2002; Kurz et al., 2008; Running, 2008). Observational studies have shown windstorms account for over 50% tree mortality across Amazonia, at scales ranging from individual trees (Esquivel-Muelbert et al., 2020) to large forest gaps exceeding thousands of hectares (ha) (Chambers et al., 2013; Negrón-Juárez et al., 2018). These wind-related tree mortality events (windthrows, also known as blowdowns) have been observed to be fan-shaped, where trees are fallen, mostly uprooted, and leaf-less (Garstang et al., 1998; Nelson et al., 1994). Windthrows can affect regional carbon cycling, and the tree mortality emphasizes the heterogeneity of the Amazon forests (Chambers et al., 2013; Espírito-Santo et al., 2010, 2014). Despite its importance, the convective characteristics producing these events remains unclear.

Windthrows can be produced by squall lines (Garstang et al., 1998; Negrón-Juárez et al., 2010) and severe precipitation events as those produced by mesoscale convective systems (MCSs) (Negrón-Juárez et al., 2018). Warm and moist air in the troposphere over tropics provides a favorable environment for the formation of MCSs (Singh et al., 2017). Rehbein et al. (2018) estimated that 7,200 continental MCSs occurred per year in the Amazonia. MCSs contribute 50%–90% of annual precipitation in the tropics (Rehbein et al., 2018; Schumacher & Rasmussen, 2020). Several studies defined criteria for identifying MCSs: a threshold between 235 and 273 K was selected to define the cold cloud top of the MCSs (Liu et al., 2008; Nunes et al., 2016; Rehbein et al., 2018; Vila et al., 2008). The average life span of MCSs is 6 hr over the Amazonia, but it can vary between short-lived systems (3–5.5 hr, account for 64% of total occurrences) and long-lived systems (over 6 hr) (Rehbein et al., 2018). Observations of MCSs in the central Amazonia area have shown that these systems are accompanied by a sudden

Writing – review & editing: Yanlei Feng, Robinson I. Negrón-Juárez, John C. H. Chiang, Jeffrey Q. Chambers

increase of wind associated with precipitation, sharp decrease in temperature, and jump in surface pressure (Garstang et al., 1998).

Although MCSs (Coniglio & Stensrud, 2004; Corfidi, Coniglio, et al., 2016; Johns & Hirt, 1986) and tree mortality (Aleixo et al., 2019; Chambers et al., 2013; Esquivel-Muelbert et al., 2020; Fontes et al., 2018) have been well studied separately, few studies focused on the mechanistic linkages between MCSs and tree mortality, a process that is currently missing in Earth System Models (ESMs). Wind-driven tree mortality has not been included in ESMs and it is an indispensable part in modeling forest dynamics in Amazonia under the current changing climate system. It can also greatly improve the connections of land and atmosphere and reduce model uncertainties in key processes, including tree mortality, carbon loss, and ecosystem resilience. Previous studies have only focused on the general pattern of windthrows and extreme precipitation events as the representation of MCSs (Espírito-Santo et al., 2010; Feng et al., 2023; Negrón-Juárez et al., 2018; Nelson et al., 1994). Yet, few studies have been conducted relating individual MCSs with windthrows on a case by case basis over the whole Amazon. Moreover, except for the general pattern of precipitation (Negrón-Juárez et al., 2018) and convective available potential energy (CAPE) (Feng et al., 2023), the relationship between other characteristics of MCSs and windthrows distribution has never been explored.

Here we developed a fusion of multiple satellite data with varying spatial and temporal resolution to study the linkages of individual large windthrow (>37 ha) with the MCSs that produced them. Our objectives are:

(1) to determine the time of windthrow occurrence, and quantify the storm passing time, cloud top brightness temperature, and precipitation of their associated MCSs;
(2) to investigate whether there are relationships between the size of windthrows and the variables quantified.

2. Methods

2.1. Correlating the MCS With Each Windthrow Event

We manually digitized 1,012 vectors of windthrows appearing on Landsat images in 2019. Due to the fact that the accurate occurrence time of these digitized windthrows is unknown, we use a fusion of land and meteorological satellites, including USGS Landsat 5,7, 8 TOA Reflectance (hereafter Landsat, 1985–2019), MOD09GA.006 Terra Surface Reflectance Daily Global 500 m (hereafter MODIS, 2000–2019), TRMM 3B42 3-Hourly Precipitation Estimates (hereafter TRMM, 1998–2019), Geostationary Operational Environmental Satellite 8, 9, 10, 11, 12, 13, 15, 16 (hereafter GOES, 1994–2019) to identify the accurate occurrence time of windthrows and find the corresponding MCSs based on the time of the windthrow. Detailed description of study area and remote sensing data sets used in this research can be found in Texts S1 and S2 in Supporting Information S1. A detailed workflow with an example for the windthrow identification process can be found in Text S3 and Figure S3 in Supporting Information S1.

There are four major steps to identify the occurrence date and time of windthrow. First, we narrowed the search of the windthrow occurrence time period by using Landsat 5, 7, 8 images. Since Landsat satellites have a 16-day repeat cycle, this provides a specific date range for each windthrow based on when the windthrow was first identified in the Landsat image, as compared to the last image where the windthrow was not present. Second, the search for the windthrow occurrence date was further narrowed to a few days using the same method with MODIS data because of the high temporal resolution of MODIS. Since MODIS has low spatial resolution of 500 m, small windthrows under ∼30 ha were impossible to identify on MODIS data. Third, we plotted the time series of TRMM precipitation estimates every 3 hr. The maximum of average precipitation over the windthrow region (a hand-drawing polygon covering each windthrow area) was calculated every 3 hr. We used TRMM precipitation to determine the day of the MCSs (Jaramillo et al., 2017; Negrón-Juárez et al., 2018) that caused these windthrow disturbances. Ideally, the date of windthrows can be easily identified if there is only one precipitation event during the few days identified by previous step. GOES data can help identify the date of windthrows if there are two precipitation events. Cases with three or more precipitation events within the time periods identified in the previous steps were not considered due to large identification uncertainty. Fourth, we plotted GOES infrared band which represents cloud top brightness temperature (hereafter cloud top temperature) over the windthrow region during the occurrence day which was identified in previous steps to identify the storm passing time. The onset of the MCSs was identified by a drop from the average cloud top temperature, and the MCSs offset was identified by a process with returning to average cloud top temperature. The average cloud top temperature for each windthrow location is calculated as the average cloud top temperature over the month when the windthrow occurs. We used

19448007, 2023, 12, Downloaded from https://agupubs.onlinelibrary.wiley.com/doi/10.1029/2023GL104395, Wiley Online Library on [06/10/2023]. See the Terms and Conditions (https://onlinelibrary.wiley.com/terms-and-conditions) on Wiley Online Library for rules of use; OA articles are governed by the applicable Creative Commons License

19448007, 2023, 12, Downloaded from https://agupubs.onlinelibrary.wiley.com/doi/10.1029/2023GL104395, Wiley Online Library on [06/10/2023]. See the Terms and Conditions (https://onlinelibrary.wiley.com/terms-and-conditions) on Wiley Online Library for rules of use; OA articles are governed by the applicable Creative Commons License

GOES data in 2019 to calculate average cloud top temperature because the data is easily accessible. The average cloud top temperature varies by location, but the general average cloud top temperature is within 245–270 K range.

We applied these four steps on a total of 157 windthrows. Windthrows were selected from large (area larger than 100 ha), medium (area between 50 and 100 ha), to small size (area smaller than 50 ha) since big windthrows were easier to identify in MODIS. We could not identify the windthrow occurrence date with windthrows smaller than ∼30 ha, as they are invisible in MODIS images. In total, we have found 38 MCSs data set grids that exactly match with the windthrow data set grids. We do not find enough cloud-free Landsat or MODIS images to identify the occurrence dates of other 119 windthrows. Following the workflow, we identified the occurrence date of 38 MCSs and associated 38 windthrows (Table S1 in in Supporting Information S1). There were 29 cases with only one precipitation event during the time period identified in step 2. There were 9 cases which had two precipitation events during the period, so we identified the onset date of MCSs by plotting GOES cloud top temperature during the time range identified in previous steps.

Amazonia encompasses Ecuador, Peru, Colombia, and Brazil. In our analysis, we divided the region into west (west of −68°), central-west (between −68° and −62°), and central-east (between −62° and −55°).

2.2. Analyzing MCS Characteristics

Once the date of the MCS occurrence was identified, we analyzed the meteorological variables of MCS, including the number of hours the MCS affecting the windthrow region (hereafter storm passing over time), coldest cloud top temperature during the time the storm passing over the region, and maximum precipitation intensity over the time the storm passing over the region. We plotted the 24 hr-time series of spatial average of GOES data over the windthrow area, which cover 12 hr before and after the MCS occurrence time derived from TRMM; we also generated the timelapse of the MCS cloud top temperature changes using GOES data (Figure S4 in Supporting Information S1) on Google Earth Engine (Gorelick et al., 2017). The storm passing over time records the total time that cloud top temperature over the windthrow area lower than the average cloud top temperature of that area. The calculation of the storm passing over time starts with the onsite time point which meet two requirements: the cloud top temperature at the time is higher than the average cloud top temperature, and the cloud top temperature at the next time point is lower than the average cloud top temperature, indicating the sharp decrease of cloud top temperature. The storm passing over time ends with the first time point where cloud top temperature climbs over the average temperature (Figure S5 in Supporting Information S1). The duration between the start and the end is calculated as the storm passing over time. The lowest cloud top temperature during this affected time period and the maximum precipitation identified using TRMM data sets were also documented for each MCSs.

3. Results

3.1. Windthrow Size and Occurrence

The smallest windthrow in the 38 windthrow cases in this study is 37 ha, and the largest windthrow is 1,468 ha (Figure S6a in Supporting Information S1). 14 windthrows are smaller than 200 ha. Based on the gap size probability distribution function in Chambers et al. (2013), large windthrows over 37 ha in this study account for less than 0.1% tree mortality in the Amazon forests.

In these 38 cases, five cases occurred in 2008, and four cases occurred in 2017, followed by three cases in 2004, 2009, 2010, and 2015 (Figure S6b in Supporting Information S1). MCSs over the Amazonia are known to occur mostly during austral summer months (Rehbein et al., 2018). In 38 cases analysis, 76% of the MCSs that caused the large windthrows happened in August (26%) and September (50%), at the transition from drier condition in austral winter to wetter condition in austral summer in western and central Amazonia (Figure S6c in Supporting Information S1). Previous study show that surface warming and moistening reduce convective inhibition energy (CINE) from this dry to wet transition period, and the weakening of CINE encourages the start of a long period of convection in the following wet season (Fu et al., 1999).

3.2. Duration of MCSs and the Size Distribution of Windthrows

A positive correlation was found between the duration of MCSs and the size of windthrows. Large windthrows in western Amazonia result from long storm passing over time (Figures 1a and 1b). There is a linear relationship

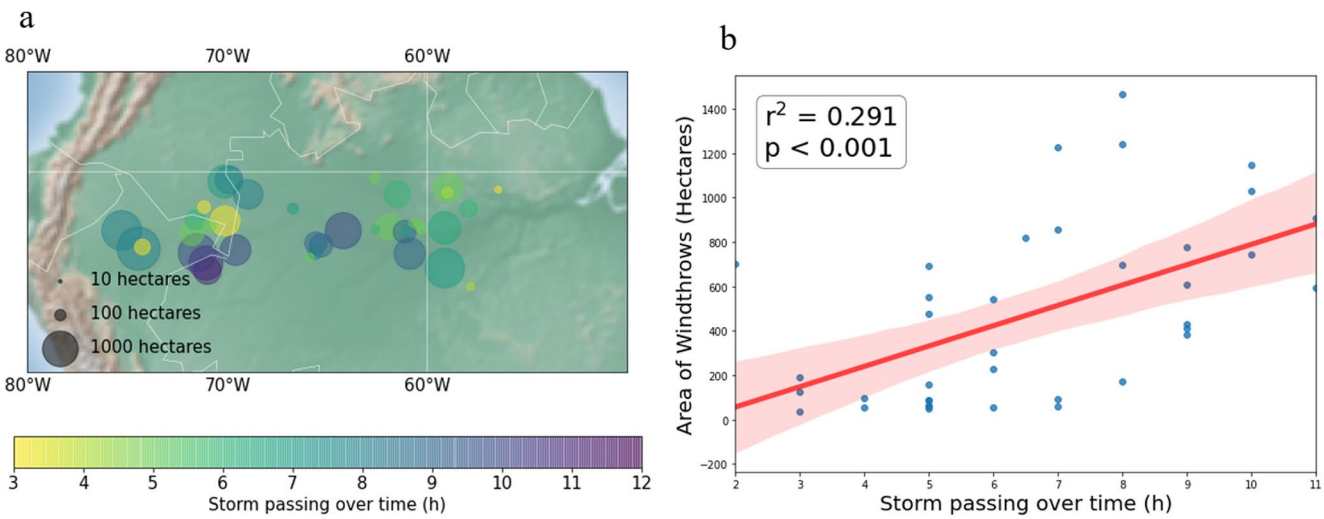

Figure 1. (a) Windthrow size and storm passing over time of associated mesoscale convective systems (MCSs). Each circle represents a case of windthrow, and the size of the circle indicates the area of disturbed forests. The color of the circle represents the storm passing over time of MCSs. Dark colors such as blue and purple indicate long hours and light color in yellow indicates relatively short hours; (b) Relationship between the duration of MCSs and area of windthrows with a 95% confidence interval.

between the duration of MCSs and the size of windthrows (Figure 1b, $r^2 = 0.291$, $p < 0.001$). In our analysis, over half of windthrows that experience over 7 hr of MCSs are in the western Amazonia (Figure 1a). Large windthrows can be related to short-lived MCSs in the western Amazon, but similar situation is not found in other region of the Amazon forests. It is worth noting that this linear relationship has large variance because the area of windthrows may be also driven by other factors such as forest resistance, wind direction, accumulated precipitation, etc. (Negron-Juarez et al., 2023).

3.3. Coldest Cloud Top Temperature of MCSs and the Size Distribution of Windthrows

Cloud top temperature of MCSs is related to cloud height since in the troposphere, air temperature decreases with increasing height (Matuura et al., 1986). Therefore, cloud top temperature can be used as a proxy for cloud height (Sherwood et al., 2004). Clouds with colder cloud top temperature are associated with tall and thick deep convective clouds, whereas relatively warm cloud top temperature can be an indicator of shallow clouds (hereafter shallow convections). Deep convections with mean coldest cloud top temperature near 206 K in Amazonia resulted in large forest disturbance, with a mean of 687 ha. Shallow convections with warm cloud top temperature higher than 230 K result in relatively small windthrows with a mean of 287 ha. There is a negative relationship between coldest cloud top temperature and the size of windthrow in western Amazonia ($r^2 = 0.3$, $p < 0.05$, sample size = 13, Figure S7 in Supporting Information S1). In general, deep convections with tall cloud are more vigorous than the shallow convections; therefore, shallow convections are associated with small forest disturbance area, with exceptions on western Amazonia due to fast forest turnover rate.

Figure 2 shows that western Amazonia had five shallow convection events (coldest cloud top temperature higher than 225 K) and caused a total of 2,237 ha of impacted forests (with a mean forest disturbance area of 447 ha). Central-west Amazonia had no shallow convection events. Central-east Amazonia had four shallow convection events and a total of 733 ha (with a mean forest disturbance area of 183 ha) of forests were affected. Shallow convection events had significant effects on forest in western Amazon, causing an area of windthrow nearly three times bigger than that in other regions; however, shallow convections have negligible impact over the central-west Amazonia and small impacts in central-east Amazonia.

3.4. TRMM Precipitation Intensity and the Forest Disturbance Size Distribution

Satellite-detected precipitation intensity associated with MCSs ranges from 0.75 to 21.78 mm/hr. Each MCS we analyzed was accompanied by precipitation, but the precipitation distribution was not uniform over all windthrow

19448007, 2023, 12, Downloaded from https://agupubs.onlinelibrary.wiley.com/doi/10.1029/2023GL104395, Wiley Online Library on [06/10/2023]. See the Terms and Conditions (https://onlinelibrary.wiley.com/terms-and-conditions) on Wiley Online Library for rules of use; OA articles are governed by the applicable Creative Commons License

19448007, 2023, 12, Downloaded from https://agupubs.onlinelibrary.wiley.com/doi/10.1029/2023GL104395, Wiley Online Library on [06/10/2023]. See the Terms and Conditions (https://onlinelibrary.wiley.com/terms-and-conditions) on Wiley Online Library for rules of use; OA articles are governed by the applicable Creative Commons License

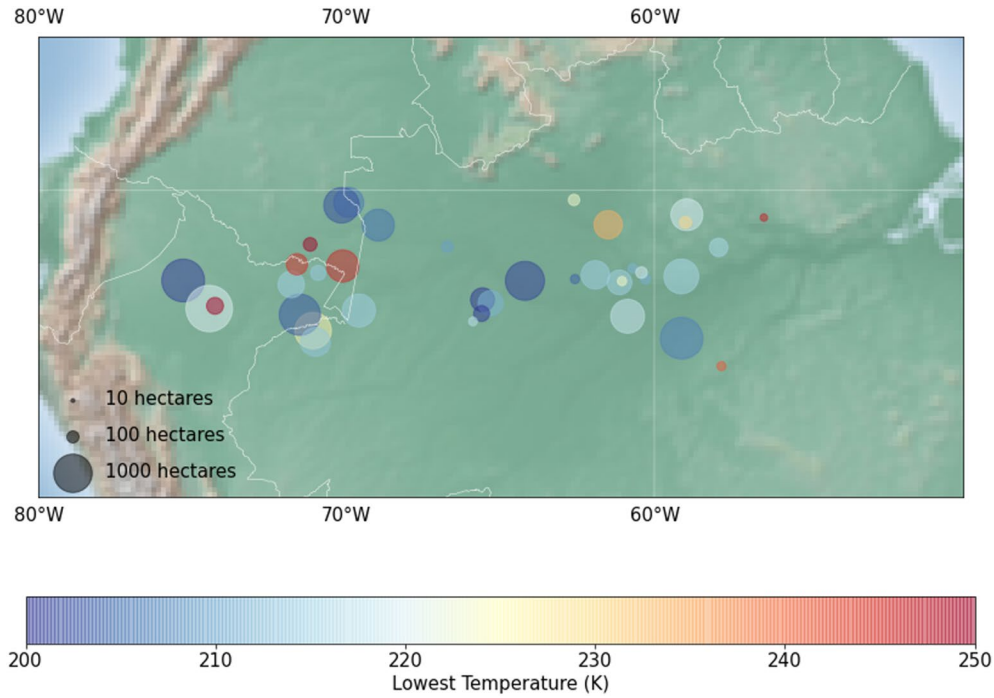

Figure 2. Windthrow sizes and the coldest temperature of associated mesoscale convective systems cloud top temperature. Circle sizes represent the areas of windthrows, and the colors indicate the temperature. Red color indicates relatively warm cloud top temperature while blue color indicates relatively cold temperature.

cases within Amazonia. The greatest precipitation occurred in western and central-west Amazonia; the central Amazonia is devoid of heavy precipitation. In the 38 case studies, 10 MCSs events were accompanied with precipitation over 10 mm per hour and a great difference was found in the corresponding windthrow sizes, ranging from 56 to 1,239 ha. No significant correlation was found between maximum hourly precipitation and the area of windthrows (Figure 3), and similar conclusion was found between accumulated precipitation during the MCSs and the area of windthrows (Figure S8 in Supporting Information S1).

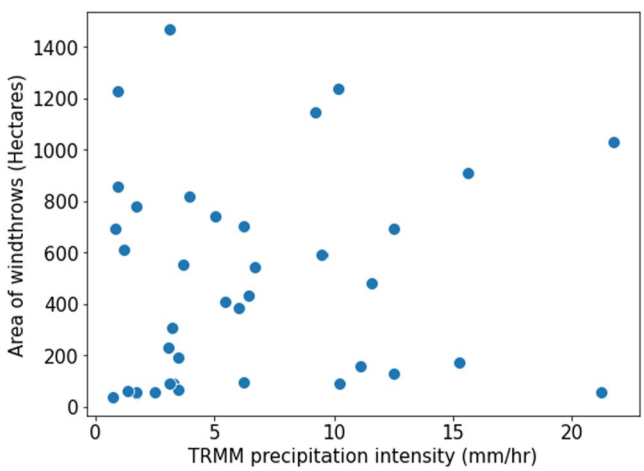

Figure 3. The relationship between the area of windthrows and precipitation intensity within area affected by mesoscale convective systems.

4. Discussion

MCSs are important drivers of tree mortality not only in Amazonia but also in US (Taeroe et al., 2019), Russia (Ulanova, 2000), Europe (Lindroth et al., 2009), and other regions (Suzuki et al., 2019). Climate system warming projects a weakening of weak MCSs but more frequent extreme MCSs (Rasmussen et al., 2020), which are the causes for large windthrows analyzed in this study (Feng et al., 2023). Therefore, it is a critical time to understand the interactions between large windthrows and MCSs. However, challenges remain in conducting analysis in this type of research because of (a) the lack of precise occurrence time of the MCSs events that caused the windthrows prevents researchers from doing case level interaction studies; therefore, previous study could only focus on the general windthrow pattern and MCSs separately; (b) the mechanism of the MCSs that directly interact with forest surface.

In this research, we have used a fusion of land surface and meteorological satellites to identify the occurrence time of 38 cases of storm-windthrow pairs and study the interaction between meteorological variables of MCSs and windthrow sizes. These 38 cases can be valuable data sets for simulation

19448007, 2023, 12, Downloaded from https://agupubs.onlinelibrary.wiley.com/doi/10.1029/2023GL104395, Wiley Online Library on [06/10/2023]. See the Terms and Conditions (https://onlinelibrary.wiley.com/terms-and-conditions) on Wiley Online Library for rules of use; OA articles are governed by the applicable Creative Commons License

tests on the wind-forest canopy interaction and for further model parameterization in ESMs to improve land-atmosphere coupling.

Our results show that these 38 cases occurred mostly in August and September in west, central-west, and central-east Amazon. Over the equatorial Amazon, high frequency of MCSs is all year around due to a warmer land surface, which is represented by high CAPE (Singh et al., 2017). The seasonal changes of MCSs occurrence are controlled by CINE and proper dynamic conditions (Rasmussen et al., 2020). Previous study show that a long wet season occurs in the west part starting from austral spring, and the frequency of convections increases starting from austral spring and reach its maximum in austral fall in Amazonia region (Fu et al., 1999). It is possible that the MCSs in the transition from dry to wet season can have more impacts on forests after experiencing several months of dry season, but it needs more support from the studies of the seasonal pattern of windthrow disturbances. It is possible that there would be more storm-windthrow pairs in wet season but frequent MCSs which represented by the high proportion of cloud cover on Landsat images prevent us from identifying more cases in wet season.

In summary, we have explored the relationship between windthrow disturbance and the corresponding MCSs. We found a positive correlation between the storm passing over time of MCS and the size of forest disturbance. This finding complements previous research on the positive correlation between the expansion rate of MCSs and their lifespan (Rehbein et al., 2018). The long storm passing over time indicates that MCSs might have lower propagation speed, producing more precipitation as they move forward (Coniglio & Stensrud, 2004; Corfidi, Coniglio, et al., 2016). Increase in associated extreme precipitation with deep convections were observed in US under global warming (Prein, Liu, et al., 2017; Prein, Rasmussen, et al., 2017), which could increase future tree mortality. It is worth noting that there is a significant spread in the linear relationship in Figure 1b, and regional variation caused by species and function traits (Aleixo et al., 2019), soil condition, and surface elevation (Negron-Juarez et al., 2023) can be important factors also affect the relationship.

We also showed that deep convections are associated with relatively large area of forest mortality, and shallow convections are associated with low to medium size of forest disturbance, depending on different sections of Amazonia. In another words, very deep MCSs with thick and high convective clouds can have very low cloud top temperatures because they have very strong updrafts (Anabor et al., 2008; Salio et al., 2007). Size expansion or shrinkage of MCSs is linearly correlated with cloud top temperature variation (Vila et al., 2008). Similar results were found in Figure S9 (in Supporting Information S1) that coldest cloud top temperature has a negative correlation with the storm passing over time of MCSs. Such deep MCSs with low cloud top temperature may come with strongest wind and heaviest precipitation, which produced more windthrow damages (Schumacher & Rasmussen, 2020).

Our results show that both hourly maximum and accumulated precipitation were not well-correlated with the size of windthrow. The lack of relationship between precipitation and windthrow size could result from dry downburst, which are less common over the Amazonia but can occur at the end of dry season (Garstang et al., 1998). Extensive precipitation, lightning, and hail are less frequently observed with these dry downbursts (Garstang et al., 1998). However, the studies on dry downburst are very limited, and this study could be used as a start for more seasonal pattern studies in MCSs in the Amazonia. On the other hand, the lack of relationship between precipitation and windthrow size could also result from the spatial and temporal resolution mismatch between TRMM precipitation data set and windthrow data sets. TRMM precipitation data set pixel is 0.25 by 0.25° (~77,000 ha), while windthrow sizes in this research range from 5–1,000 ha. The spatial average of TRMM precipitation over the 0.25 by 0.25 pixel may result in the underestimate of MCS precipitation used in this study. Moreover, TRMM precipitation data were captured as snapshots considered to represent the 3-hr period. It is very likely the time of the snapshot does not match the time of the MCS maximum precipitation, given the fact that over half of MCSs last less than 6 hr (Rehbein et al., 2018). Therefore, even the maximum of TRMM precipitation can still be much lower than actual MCS precipitation intensity. Precipitation data at higher spatial and temporal resolution from flux towers in Amazonia may help aid the analysis in the future.

In addition to precipitation, further analysis can be done to investigate how downdraft gust, strength of resulting straight-line winds, the extent of surface area affected by damaging winds, the size, convective mode of the MCS, duration and forward speed of the MCS determine the size of windthrow (Corfidi, Coniglio, et al., 2016; Corfidi, Johns, et al., 2016; Johns & Hirt, 1987). To the extent that the duration and depth of convection is tied to surface winds generated by MCSs (Garstang et al., 1998; Oliveira et al., 2020), our findings build the connection between

19448007, 2023, 12, Downloaded from https://agupubs.onlinelibrary.wiley.com/doi/10.1029/2023GL104395, Wiley Online Library on [06/10/2023]. See the Terms and Conditions (https://onlinelibrary.wiley.com/terms-and-conditions) on Wiley Online Library for rules of use; OA articles are governed by the applicable Creative Commons License

land surfaces and descending winds. The results also shed lights for future research in regional-scale carbon and water fluxes between the atmosphere and biosphere and improvements in global ESMs.

The relatively bigger size of windthrows created by shallow convections in western Amazonia compared to other parts of Amazonia indicates that forests in western Amazonia are more vulnerable to MCSs. There are two main reasons: wood density and soil. Compared to forests in central and central west Amazonia, forests in western Amazonia have lower wood density, relative slower growth rate, higher recruitment rates that related to higher tree-mortality, and these characteristics make them more vulnerable to MCSs (Baker et al., 2004; Chao et al., 2008; Ter Steege et al., 2006). In austral spring and fall, warmer land surface, more humid lower troposphere, and weak inversion in western Amazonia lead to high frequency of MCSs (Fu et al., 1999). Convections with relative warm cloud top have non-negligible impacts on forests in western Amazonia. This negative feedback loop between forests in western Amazonia and MCSs complements similar conclusions of the previous studies (Negrón-Juárez et al., 2018; Stephenson et al., 2011). Soil fertility is another indicator of adult tree growth (Ter Steege et al., 2006). Soils in western Amazonia limit root growth and result in rapid vertical growth and shallow root system, while soils in central Amazonia allow the development of deeper root (Negrón-Juárez et al., 2018; Quesada et al., 2012; Stephenson et al., 2011). Shallow root system of forests in western Amazonia limit the anchoring ability of trees into soil; therefore, they are more sensitive to MCSs than forests with deeper roots (Negrón-Juárez et al., 2018).

5. Conclusion

In this study, we use 38 cases of windthrow and their matched MCSs events to analyze how features of individual MCSs affect the size of windthrows. We find that MCSs with long storm passing over time result in large windthrows, and there is a positive correlation between the duration of MCSs and the size of windthrow. MCSs with deep convections result in large windthrows across the entire Amazon; shallow convections can cause medium size windthrows in west Amazonia and result in small windthrows in central Amazonia. We also find that TRMM precipitation is not uniform among forest disturbances with the same size, and precipitation data with higher spatial and temporal resolution is needed to investigate a clearer relationship with windthrow sizes. Our research provides detailed case studies of windthrows in Amazonia and the corresponding MCS features, which can reduce the uncertainty brought by MCSs and windthrow data mismatch in the previous studies and bring new insights on the interactions of land surface and atmosphere in ESMs.

Data Availability Statement

All the source data used in this study can be freely download from public repositories. Landsat 5, 7, 8 courtesy of the U.S. Geological Survey, TRMM precipitation data courtesy of NASA were available on Google Earth Engine platform (GEE) (Gorelick et al., 2017). GEE requires registration to obtain a free account, then Landsat 5 (https://developers.google.com/earth-engine/datasets/catalog/LANDSAT_LT05_C01_T1_TOA), 7 (https://developers.google.com/earth-engine/datasets/catalog/LANDSAT_LE07_C01_T1_TOA), 8 (https://developers.google.com/earth-engine/datasets/catalog/LANDSAT_LC08_C01_T1_TOA), TRMM (https://developers.google.com/earth-engine/datasets/catalog/TRMM_3B42) can be found in the search bar and easily imported into the GEE code platform for analysis. GEE code example to analyze windthrows is available at https://github.com/ylfeng93/windthrow_cases. Archive GOES data can be downloaded at https://inventory.ssec.wisc.edu/inventory/#search. Free registration is required to get a valid API key. Using keywords, including latitude, longitude, date, satellite name, coverage, GOES images with band at 10.1–10.7 μm (band 4 of GOES 8, 12, 13, and band 13 of GOES 16) at the locations of 38 cases were downloaded. The unit of each pixel value is temperature. The detailed tutorial for downloading archived GOES data can be found at https://mcfetch.ssec.wisc.edu/#tutorial. All data analysis conduct for this project was undertaken using freely available software in QGIS version 3.24 (https://qgis.org/en/site/forusers/download.html#) or Python version 3.10.4 (https://www.python.org/downloads/).

Acknowledgments
This work was supported as part of the Next Generation Ecosystem Experiments-Tropics (NGEE Tropics), funded by the US Department of Energy, Office of Science, Office of Biological and Environmental Research under award no. DE-AC02-05CH11231. We are grateful to the Satellite Data Service (SDS) group at the University of Wisconsin-Madison Space Science and Engineering Center (SSEC) for access, maintenance, and distribution of archive GOES data.

References

Aleixo, I., Norris, D., Hemerik, L., Barbosa, A., Prata, E., Costa, F., & Poorter, L. (2019). Amazonian rainforest tree mortality driven by climate and functional traits. *Nature Climate Change*, *9*(5), 384–388. https://doi.org/10.1038/s41558-019-0458-0

Anabor, V., Stensrud, D. J., & De Moraes, O. L. L. (2008). Serial upstream-propagating mesoscale convective system events over southeastern South America. *Monthly Weather Review*, *136*(8), 3087–3105. https://doi.org/10.1175/2007MWR2334.1

Baccini, A., Walker, W., Carvalho, L., Farina, M., Sulla-Menashe, D., & Houghton, R. A. (2017). Tropical forests are a net carbon source based on aboveground measurements of gain and loss. *Science*, *358*(6360), 230–234. https://doi.org/10.1126/science.aam5962

Baker, T. R., Phillips, O. L., Malhi, Y., Almeida, S., Arroyo, L., Di Fiore, A., et al. (2004). Variation in wood density determines spatial patterns in Amazonian forest biomass. *Global Change Biology*, *10*(5), 545–562. https://doi.org/10.1111/j.1365-2486.2004.00751.x

Baldocchi, D. (2008). "Breathing" of the terrestrial biosphere: Lessons learned from a global network of carbon dioxide flux measurement systems. *Australian Journal of Botany*, *56*(1), 1–26. https://doi.org/10.1071/BT07151

Chambers, J. Q., Negron-Juarez, R. I., Marra, D. M., Di Vittorio, A., Tews, J., Roberts, D., et al. (2013). The steady-state mosaic of disturbance and succession across an old-growth central Amazon forest landscape. *Proceedings of the National Academy of Sciences of the United States of America*, *110*(10), 3949–3954. https://doi.org/10.1073/pnas.1202894110

Chao, K. J., Phillips, O. L., Gloor, E., Monteagudo, A., Torres-Lezama, A., & Martínez, R. V. (2008). Growth and wood density predict tree mortality in Amazon forests. *Journal of Ecology*, *96*(2), 281–292. https://doi.org/10.1111/j.1365-2745.2007.01343.x

Coniglio, M. C., & Stensrud, D. J. (2004). Interpreting the climatology of derechos. *Weather and Forecasting*, *19*(3), 595–605. https://doi.org/10.1175/1520-0434(2004)019<0595:ITCOD>2.0.CO;2

Corfidi, S. F., Coniglio, M. C., Cohen, A. E., & Mead, C. M. (2016). A proposed revision to the definition of "derecho". *Bulletin of the American Meteorological Society*, *97*(6), 935–949. https://doi.org/10.1175/BAMS-D-14-00254.1

Corfidi, S. F., Johns, R. H., & Darrow, M. A. (2016). The Great Basin derecho of 31 May 1994. *Weather and Forecasting*, *31*(3), 917–935. https://doi.org/10.1175/WAF-D-15-0178.1

Cox, P. M., Pearson, D., Booth, B. B., Friedlingstein, P., Huntingford, C., Jones, C. D., & Luke, C. M. (2013). Sensitivity of tropical carbon to climate change constrained by carbon dioxide variability. *Nature*, *494*(7437), 341–344. https://doi.org/10.1038/nature11882

Espírito-Santo, F. D. B., Gloor, M., Keller, M., Malhi, Y., Saatchi, S., Nelson, B., et al. (2014). Size and frequency of natural forest disturbances and the Amazon forest carbon balance. *Nature Communications*, *5*, 1–6. https://doi.org/10.1038/ncomms4434

Espírito-Santo, F. D. B., Keller, M., Braswell, B., Nelson, B. W., Frolking, S., & Vicente, G. (2010). Storm intensity and old-growth forest disturbances in the Amazon region. *Geophysical Research Letters*, *37*(11), 1–6. https://doi.org/10.1029/2010GL043146

Esquivel-Muelbert, A., Phillips, O. L., Brienen, R. J. W., Fauset, S., Sullivan, M. J. P., Baker, T. R., et al. (2020). Tree mode of death and mortality risk factors across Amazon forests. *Nature Communications*, *11*(1), 5515. https://doi.org/10.1038/s41467-020-18996-3

Feng, Y., Negrón-Juárez, R. I., Romps, D. M., & Chambers, J. Q. (2023). Amazon windthrow disturbances are likely to increase with storm frequency under global warming. *Nature Communications*, *14*(1), 2–9. https://doi.org/10.1038/s41467-022-35570-1

Fontes, C. G., Chambers, J. Q., & Higuchi, N. (2018). Revealing the causes and temporal distribution of tree mortality in Central Amazonia. *Forest Ecology and Management*, *424*(April), 177–183. https://doi.org/10.1016/j.foreco.2018.05.002

Fu, R., Zhu, B., & Dickinson, R. E. (1999). How do atmosphere and land surface influence seasonal changes of convection in the tropical Amazon? *Journal of Climate*, *12*(5 I), 1306–1321. https://doi.org/10.1175/1520-0442(1999)012<1306:HDAALS<2.0.CO;2

Garstang, M., White, S., Shugart, H. H., & Halverson, J. (1998). Convective cloud downdrafts as the cause of large blowdowns in the Amazon rainforest. *Meteorology and Atmospheric Physics*, *67*(1–4), 199–212. https://doi.org/10.1007/BF01277510

Gatti, L. V., Basso, L. S., Miller, J. B., Gloor, M., Gatti Domingues, L., Cassol, H. L. G., et al. (2021). Amazonia as a carbon source linked to deforestation and climate change. *Nature*, *595*(7867), 388–393. https://doi.org/10.1038/s41586-021-03629-6

Gorelick, N., Hancher, M., Dixon, M., Ilyushchenko, S., Thau, D., & Moore, R. (2017). Google Earth Engine: Planetary-scale geospatial analysis for everyone. *Remote Sensing of Environment*, *202*, 18–27. https://doi.org/10.1016/j.rse.2017.06.031

Jaramillo, L., Poveda, G., & Mejía, J. F. (2017). Mesoscale convective systems and other precipitation features over the tropical Americas and surrounding seas as seen by TRMM. *International Journal of Climatology*, *37*, 380–397. https://doi.org/10.1002/joc.5009

Johns, R. H., & Hirt, W. D. (1986). Derechos: Widespread convectively induced windstorms. *Weather and Forecasting*, *2*, 32–49. https://doi.org/10.1175/1520-0434(1987)002<0032:dwciw>2.0.co;2

Johns, R. H., & Hirt, W. D. (1987). Derechos: Widespread convectively induced windstorms. *Weather and Forecasting*, *2*(1), 32–49. https://doi.org/10.1175/1520-0434(1987)002<0032:dwciw>2.0.co;2

Knohl, A., Kolle, O., Minayeva, T. Y., Milyukova, I. M., Vygodskaya, N. N., Foken, T., & Schulze, E. D. (2002). Carbon dioxide exchange of a Russian boreal forest after disturbance by wind throw. *Global Change Biology*, *8*(3), 231–246. https://doi.org/10.1046/j.1365-2486.2002.00475.x

Kurz, W. A., Stinson, G., Rampley, G. J., Dymond, C. C., & Neilson, E. T. (2008). Risk of natural disturbances makes future contribution of Canada's forests to the global carbon cycle highly uncertain. *Proceedings of the National Academy of Sciences of the United States of America*, *105*(5), 1551–1555. https://doi.org/10.1073/pnas.0708133105

Lindroth, A., Lagergren, F., Grelle, A., Klemedtsson, L., Langvall, O., Weslien, P., & Tuulik, J. (2009). Storms can cause Europe-wide reduction in forest carbon sink. *Global Change Biology*, *15*(2), 346–355. https://doi.org/10.1111/j.1365-2486.2008.01719.x

Liu, C., Zipser, E. J., Cecil, D. J., Nesbitt, S. W., & Sherwood, S. (2008). A cloud and precipitation feature database from nine years of TRMM observations. *Journal of Applied Meteorology and Climatology*, *47*(10), 2712–2728. https://doi.org/10.1175/2008JAMC1890.1

Matuura, N., Masuda, Y., Inuki, H., Kato, S., Fukao, S., Sato, T., & Tsuda, T. (1986). Radio acoustic measurement of temperature profile in the troposphere and stratosphere. *Nature*, *323*(6087), 426–428. https://doi.org/10.1038/323426a0

Mitchard, E. T. A. (2018). The tropical forest carbon cycle and climate change. *Nature*, *559*(7715), 527–534. https://doi.org/10.1038/s41586-018-0300-2

Negron-Juarez, R., Magnabosco-Marra, D., Feng, Y., Urquiza-Muñoz, J. D., Riley, W. J., & Chambers, J. Q. (2023). Windthrow characteristics and their regional association with rainfall, soil, and surface elevation in the Amazon. *Environmental Research Letters*, *18*(1), 014030. https://doi.org/10.1088/1748-9326/acaf10

Negrón-Juárez, R. I., Chambers, J. Q., Guimaraes, G., Zeng, H., Raupp, C. F. M., Marra, D. M., et al. (2010). Widespread Amazon forest tree mortality from a single cross-basin squall line event. *Geophysical Research Letters*, *37*(16), 1–5. https://doi.org/10.1029/2010GL043733

Negrón-Juárez, R. I., Holm, J. A., Marra, D. M., Rifai, S. W., Riley, W. J., Chambers, J. Q., et al. (2018). Vulnerability of Amazon forests to storm-driven tree mortality. *Environmental Research Letters*, *13*(5), 054021. https://doi.org/10.1088/1748-9326/aabe9f

Nelson, B. W., Kapos, V., Adams, J. B., Oliveira, W. J., Braun, O. P. G., & do Amaral, I. L. (1994). Forest disturbance by large blowdowns in the Brazilian Amazon. *Ecology*, *75*(3), 853–858. https://doi.org/10.2307/1941742

Nunes, A. M. P., Silva Dias, M. A. F., Anselmo, E. M., & Morales, C. A. (2016). Severe convection features in the Amazon basin: A TRMM-based 15-year evaluation. *Frontiers in Earth Science*, *4*(April), 1–14. https://doi.org/10.3389/feart.2016.00037

Oliveira, M. I., Acevedo, O. C., Sörgel, M., Nascimento, E. L., Manzi, A. O., Oliveira, P. E. S., et al. (2020). Planetary boundary layer evolution over the Amazon rainforest in episodes of deep moist convection at the Amazon Tall Tower Observatory. *Atmospheric Chemistry and Physics*, *20*(1), 15–27. https://doi.org/10.5194/acp-20-15-2020

Prein, A. F., Liu, C., Ikeda, K., Trier, S. B., Rasmussen, R. M., Holland, G. J., & Clark, M. P. (2017). Increased rainfall volume from future convective storms in the US. *Nature Climate Change*, *7*(12), 880–884. https://doi.org/10.1038/s41558-017-0007-7

19448007, 2023, 12, Downloaded from https://agupubs.onlinelibrary.wiley.com/doi/10.1029/2023GL104395, Wiley Online Library on [06/10/2023]. See the Terms and Conditions (https://onlinelibrary.wiley.com/terms-and-conditions) on Wiley Online Library for rules of use; OA articles are governed by the applicable Creative Commons License

Prein, A. F., Rasmussen, R. M., Ikeda, K., Liu, C., Clark, M. P., & Holland, G. J. (2017). The future intensification of hourly precipitation extremes. *Nature Climate Change*, *7*(1), 48–52. https://doi.org/10.1038/nclimate3168

Quesada, C. A., Phillips, O. L., Schwarz, M., Czimczik, C. I., Baker, T. R., Patiño, S., et al. (2012). Basin-wide variations in Amazon forest structure and function are mediated by both soils and climate. *Biogeosciences*, *9*(6), 2203–2246. https://doi.org/10.5194/bg-9-2203-2012

Rasmussen, K. L., Prein, A. F., Rasmussen, R. M., Ikeda, K., & Liu, C. (2020). Changes in the convective population and thermodynamic environments in convection-permitting regional climate simulations over the United States. *Climate Dynamics*, *55*(1–2), 383–408. https://doi.org/10.1007/s00382-017-4000-7

Rehbein, A., Ambrizzi, T., & Mechoso, C. R. (2018). Mesoscale convective systems over the Amazon basin. Part I: Climatological aspects. *International Journal of Climatology*, *38*(1), 215–229. https://doi.org/10.1002/joc.5171

Running, S. W. (2008). Ecosystem disturbance, carbon, and climate. *Science*, *321*(5889), 652–653. https://doi.org/10.1126/science.1159607

Salio, P., Nicolini, M., & Zipser, E. J. (2007). Mesoscale convective systems over southeastern South America and their relationship with the South American low-level jet. *Monthly Weather Review*, *135*(4), 1290–1309. https://doi.org/10.1175/MWR3305.1

Schumacher, R. S., & Rasmussen, K. L. (2020). The formation, character and changing nature of mesoscale convective systems. *Nature Reviews Earth & Environment*, *1*(6), 300–314. https://doi.org/10.1038/s43017-020-0057-7

Sherwood, S. C., Chae, J. H., Minnis, P., & McGill, M. (2004). Underestimation of deep convective cloud tops by thermal imagery. *Geophysical Research Letters*, *31*(11), 1–4. https://doi.org/10.1029/2004GL019699

Singh, M. S., Kuang, Z., Maloney, E. D., Hannah, W. M., & Wolding, B. O. (2017). Increasing potential for intense tropical and subtropical thunderstorms under global warming. *Proceedings of the National Academy of Sciences of the United States of America*, *114*(44), 11657–11662. https://doi.org/10.1073/pnas.1707603114

Stephenson, N. L., van Mantgem, P. J., Bunn, A. G., Bruner, H., Harmon, M. E., O'Connell, K. B., et al. (2011). Causes and implications of the correlation between forest productivity and tree mortality rates. *Ecological Monographs*, *81*(4), 527–555. https://doi.org/10.1890/10-1077.1

Suzuki, S. N., Tsunoda, T., Nishimura, N., Morimoto, J., & Suzuki, J. I. (2019). Dead wood offsets the reduced live wood carbon stock in forests over 50 years after a stand-replacing wind disturbance. *Forest Ecology and Management*, *432*, 94–101. https://doi.org/10.1016/j.foreco.2018.08.054

Taeroe, A., de Koning, J. H. C., Löf, M., Tolvanen, A., Heiðarsson, L., & Raulund-Rasmussen, K. (2019). Recovery of temperate and boreal forests after windthrow and the impacts of salvage logging. A quantitative review. *Forest Ecology and Management*, *446*(May), 304–316. https://doi.org/10.1016/j.foreco.2019.03.048

Ter Steege, H., Pitman, N. C. A., Phillips, O. L., Chave, J., Sabatier, D., Duque, A., et al. (2006). Continental-scale patterns of canopy tree composition and function across Amazonia. *Nature*, *443*(7110), 444–447. https://doi.org/10.1038/nature05134

Ulanova, N. G. (2000). The effects of windthrow on forests at different spatial scales: A review. *Forest Ecology and Management*, *135*(1–3), 155–167. https://doi.org/10.1016/S0378-1127(00)00307-8

Vila, D. A., Machado, L. A. T., Laurent, H., & Velasco, I. (2008). Forecast and tracking the evolution of cloud clusters (ForTraCC) using satellite infrared imagery: Methodology and validation. *Weather and Forecasting*, *23*(2), 233–245. https://doi.org/10.1175/2007WAF2006121.1

19448007, 2023, 12, Downloaded from https://agupubs.onlinelibrary.wiley.com/doi/10.1029/2023GL104395, Wiley Online Library on [06/10/2023]. See the Terms and Conditions (https://onlinelibrary.wiley.com/terms-and-conditions) on Wiley Online Library for rules of use; OA articles are governed by the applicable Creative Commons License